GLOBAL ACADEMIC RESEARCH INSTITUTE

COLOMBO, SRI LANKA

GARI International Journal of Multidisciplinary Research

ISSN 2659-2193

Volume: 08 | Issue: 04

On 31st December 2022

http://www.research.lk

Author: Mohamed Ifran, Heshani Mudalige, Ominda perera

School of Science, BMS, Sri Lanka

GARI Publisher | NCD | Volume: 08 | Issue: 04

Article ID: IN/ GARI/ICAS/2022/117A | Pages: 128-155 (27)

ISSN 2659-2193 | Edit: GARI Editorial Team

Received: 28.08.2022 | Publish: 31.12.2022

PROTEIN-LIGAND DOCKING STUDY FOR THE IDENTIFICATION OF BINDING SITES AND LIGANDS AGAINST THE ISCHEMIC STROKE RECEPTORS

Mohamed Ifran, Heshani Mudalige, Ominda perera

School of Science, BMS, Sri Lanka

ABSTRACT

Globally, Ischemic stroke is an onerous disease which is the foremost reason for permanent disabilities and second leading cause of morbidity. It is mediated by various pathophysiological pathways. Prevailing current treatments are restricted to anti-platelet therapy and thrombolytic agent which may pave a way to hemorrhagic condition. Antagonism for PAF-R and S1R has become a novel therapeutic strategy for ischemic stroke. Receptor and phytochemicals 3D structures were retrieved from RCSB PDB and PubChem. BD and SSD were carried out in Autodock. In vina, *.BAT file was created to execute docking for phytochemicals in a single config.txt file. Based on BE and Ki, phytocompounds were short-listed and further filtered in relevant to ADME properties including the Lipinski's rule of five, GI absorption and PAINS which were verified by SwissADME webtool. Ramachandran plot and redocking (-10.7 kcal/mol, RMSD=0.382) for 5ZKP and 5HK1 (-10.1 kcal/mol, RMSD= 0.354) were carried out for validation. Docking poses and interactions were analysed in BIOVIA DS and Ligplot+. Blazeispirol X showed best BE= -11.76 kcal/mol, Ki= 6.6 nM in AD4 SSD and vina (-12.1 kcal/mol) for 5ZKP and manoalide showed best results of (BE=-10.18 kcal/mol, Ki= 34.35 nM in AD4 SSD for 5HK1 while licoricidin showed -10.9 kcal/mol in vina. PHE 174, PHE 97, LEU 279 and TRP 73 were identified as common AARs in 5ZKP. As the most common AARs in 5HK1, MET93, ALA185, LEU182, TYR103, TYR206, and LEU495 were identified. Future research can be performed based on this study to uncover phytochemicals to treat ischemic stroke.

Key words: PAF-R, S1R, .BAT, Blazeispirol X

ABBREVIATIONS

IS : Ischemic stroke
AD4 : Autodock 4
BD : Blind docking
SSD : Site specific docking
MD : Molecular dockings
PAF-R : Platelet activating factor receptor
S1R : Sigma 1 receptor
GPF : Grid parameter file
DPF : Docking parameter file
GLG : Grid log file
DLG : Docking log file
BBB : Blood brain barrier
HB : Hydrogen bond
HPI : Hydrophobic interaction
BE : Binding energy
BA : Binding affinity
GA : Genetic Algorithm
LGA : Lamarckian genetic algorithm
AAI : Amino acids interaction
AAR : Amino acid residues
PDB : Protein Data Bank
PCA : Principal component analysis
LC-MS : liquid chromatography mass spectrophotometry

INTRODUCTION

Ischemic stroke

Stroke is an exigent disease that leads to a high morbidity, and it has developed as one of the three most ubiquitous and critical illnesses across the globe (Katan and Luft, 2018; Yang et al., 2022). Furthermore, stroke has a high disability rate, leading to perpetual disability for about half of its survivors (Donkor, 2018). Age, hypertension, obesity, hyperlipidemia, diabetes, smoking, and alcohol consumption are major risk factors linked with stroke (Kuriakose and Xiao, 2020). With the increase in the ageing population the incidence of stroke is predicted to continue increasing, and by 2030, the mortality of stroke may surpass 12% (Xing et al., 2012). Thus, stroke surges the worldwide economic and social burden (Xu et al., 2021). In general, stroke can be divided into ischemic stroke (IS) and hemorrhagic stroke (HS), based on the way the blood flow is interrupted. Hemorrhagic stroke ensues from the ruptures of a debilitated blood vessel, resulting in the accumulation of blood in the neighbouring brain tissue (Chauhan and Debette, 2016). Of the two, ischemic stroke is the main type which amounted to 87% of all strokes (Moon et al., 2021). Symptoms of IS depend upon the location where the brain damage occurs. Commonly, the symptoms are face drooping, arm weakness, slurred speech and diplopia, bulbar palsies, and dysphagia (Musuka et al., 2015). thrombolysis, mechanical thrombectomy and neuroprotective therapies are the current major treatment available for IS (Liaw and Liebeskind, 2020).

Pathophysiology of ischemic stroke

Excitotoxicity, focal cerebral ischemia, hypoxia, energy depletion, oxidative stress, neuronal apoptosis, nerve necrosis and blood-brain barrier (BBB) disruption mainly express the pathophysiological process of IS (Zhou et al., 2021; Orellana-Urzúa et al., 2020).

protein-ligand docking

Protein–ligand docking is important method to understand therapeutic utilization (Huang and Zou, 2010). The primary aim of this is to predict the conformation and orientation (binding poses) of a ligand when it binds to a protein receptor. Tertiary (3D) structures of proteins are essential to determine the functions of protein such as interactions and binding affinity. Computational docking is considered an imperative approach for study of protein-ligand interactions and for drug discovery and development (Hernández-Santoyo et al., 2013). The docking techniques can be classified as blind and site-specific docking. Blind docking is executed as the grid box covers the entire protein receptor. This method is an excellent technique for the detection of binding sites of (novel) proteins. However, being computationally slow is the drawback of this approach. Site-specific docking is performed when the binding pocket is known which is comparatively quick and accurate (Meng et al., 2011). Figure 2 depicts the summative procedure of docking

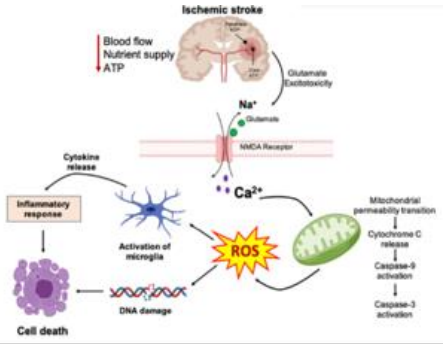

Figure 1: Pathophysiological pathways of Ischemic stroke (Barzegar et al., 2021)

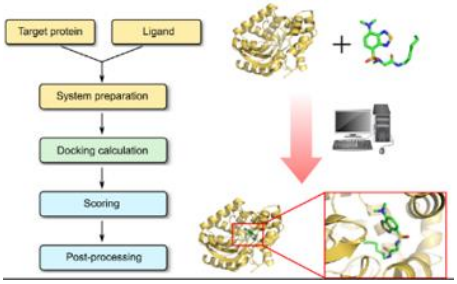

Figure 2: Steps involved in docking (Protein–Ligand Docking - Profacgen, 2022)

Protein receptor selection

Biologically active in the stable state is the main characteristics of receptors. The study focuses on proteins which are novel target for ischemic stroke in humans. The selection of target protein for docking purpose is according to their X-ray diffraction. The selected protein should be free from protein break in entire 3D conformity, and in PDB formats to encounter prerequisites of docking analysis. X-ray crystallographic structures of 5ZKP Human platelet-activating factor receptor (PAF-R) and Human Sigma-1 receptor Enzyme (S1R) are prepared for docking as shown in Table 1.

Table 1: *Details of the receptors used in the study*

Receptor	**platelet-activating factor receptor**	**Human sigma-1 receptor**
PDB ID	5ZKP	5HK1
Structure		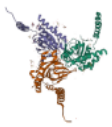
Expression system	*Spodoptera frugiperda*	
Resolution	2.81 Å	2.51 Å
Chains	A	A, B, C
Extraction method	X-ray diffraction	
Natural ligands	9ER, FMN	OLC, 61W, SO4
References	(Cao *et al.*, 2018)	(Schmidt *et al.*, 2016)

Ligand selection

Ligands must have the ability to interact with the target receptor. In this study, FDA approved drugs (Figure 3) and phytochemicals (Table2) are used as ligands based on the cost-effectiveness and effortless availability

.

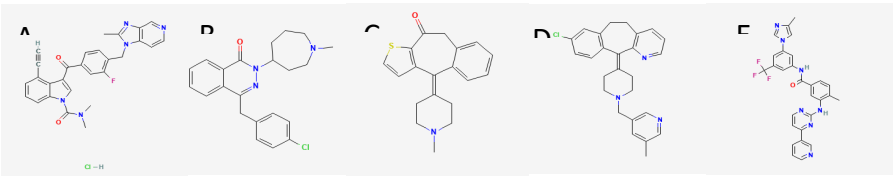

Figure 3: (A) ABT-491_HCL (B) Azelastine (C) Ketotifen (D) Rupatadine (E) Nilotinib

Table 2: Few Phytochemicals used in the study

Phytochemical	Source	References
Yangambin	*Ocotea fasciculata*	(Martins *et al.*, 2020)
Manoalide	*Luffariella variabilis*	(Nakao and Fusetani, 2010)
Kadsurenone	*Piper kadsura*	(Huang *et al.*, 2009)
Denudatin	*Hypericum denudatum*	(Bridi *et al.*, 2017)
Andrographolide	***Andrographis paniculata***	(Brahmachari, 2017)

Software utilization

AutoDock is an open-source, molecular modelling software available freely that is utilized for protein-ligand docking with high accuracy. AutoDock Vina is one of the fastest and most broadly operated open-source docking engines. It is a computational docking program that runs on a simple scoring function and rapid gradient-optimization conformational search. AD4 provides better binding site prediction with precalculated grid-maps. UCSF Chimera is an alternative advanced software platform for docking through vina and visualization of molecular structures (Butt et al., 2019; El-Hachem et al., 2017). Visualization software such as PyMOL, BIOVIA DS and LigPlot are beneficial to analyse and obtain the structures of protein complex (Laskowski and Swindells, 2011)

Validation

Redocking and superimposition are the methods used to validate the docking procedure, exclude false-positive result, and examine the productiveness (Saliu et al., 2021). Ramachandran plot can be used for assessing the precision of predicted protein structure (Agnihotry et al., 2022). As a secondary verification tool, Ramachandran plots assists to verify the stereochemistry and geometry of the complex by creating that none of the geometries are in the plot's prohibited electrostatically unfavored regions (Patil et al., 2019).

Significance of the study

IS remains the prominent reason of morbidity and mortality. Existing stroke treatment is restricted to two groups of FDA-approved drugs of thrombolytic agents (tissue plasminogen activator (tPA)) and antithrombotic agents (aspirin and heparin). After onset of stroke symptoms, these current treatments have a limited time-window (<4.5 h) for administration. While thrombolytic agents reinstate perfusion, they involve severe risks for hemorrhage, and do not influence responses for injury during reperfusion. Therefore, stroke therapies that can suppress detrimental effects of ischemic injury are vastly needed. With regard to that, PAF-R and S1R are new therapeutic approach to target IS. Arterial thrombogenesis is a crucial pathological pathway, which is regulated by PAF-R, leading to IS. Therefore, targeting PAF-R with antagonists is highly effective (Bazan et al., 2015). Ample studies suggest, sigma 1 receptor is capable of being targeted for treatment of IS (Sałaciak and Pytka, 2022).

Objectives

General objective

To select the potential and effective ligands and to identify their binding sites against IS receptor proteins and find treatment for IS.

Specific objectives

To be familiar with software such as AutoDock, AutoDock Vina, PyMOL and Chimera.

To identify the best ligand binding sites for IS receptor protein by performing blind and site-specific docking using AutoDock/Autodock Vina/Chimera.

To find the most potent FDA-approved drugs and phytochemicals against IS by targeting 5ZKP and 5HK1 receptors.

To examine the feasibility to target S1R for treatment with respect to ADME analysis.

MATERIALS AND METHODOLOGY

Materials

Table 3: *Materials of the study*

Hardware		Software	Webtools
PC with processor 11th Gen Intel(R) Core i7-1165G7@2.80GHz		Python 3.10.2	RCSB PDB (Protein Data Bank)
RAM 8.00 GB (7.70 GB usable)		MGLTools 1.5.7	NCBI PubChem
		AutoDockTools 4.2.6	SwissADME
Sample	Others	Autodock Vina 1.1.2	Ramachandran Analysis (SAVESv6.0 – Structure Validation Server (ucla.edu)
FDA approved drugs	Dialog 4G router	OpenBabel GUI 2.4.1	
		PyMOL 2.5	
		BIOVIA Discovery Studio 2021	
Phytochemicals		UCSF Chimera	
		LigPlot+ v2.2	

METHODOLOGY

Software installation

The below-mentioned software was downloaded and installed according to the user manual provided.

Table 4: *Utilized software for the study*

Software	Links	References
Python 3.10.2	https://www.python.org/	Morris, Huey and Olson, 2008.
MGLTools 1.5.7	https://ccsb.scripps.edu/mgltools/	Trott and Olson, 2009.
AutoDockTools 4.2.6	https://autodock.scripps.edu/	
Autodock Vina 1.1.2	https://vina.scripps.edu/	
OpenBabel GUI 2.4.1	https://sourceforge.net/projects/openbabel/	Laskowiski and Swindells, 2011.
PyMOL 2.5	https://pymol.org/2/	Morris, Huey and Olson, 2008.
BIOVIA Discovery Studio	https://discover.3ds.com/discovery-studio-visualizer-download	Trott and Olson, 2009.
UCSF Chimera	https://www.cgl.ucsf.edu/chimera/	
LigPlot+ v2.2	https://www.ebi.ac.uk/thornton-srv/software/LigPlus/ https://www.java.com/en/	

Familiarization of software

Computer workshops, self-study, literature survey, YouTube tutorials were exercised to obtain the basics of each software. Autodock 4.2.6 user manual and 'Workflow Docking with Autodock 4: A Beginner's Guide' by Ahamad. T (2021) were scrutinized to acquire adequate knowledge on Autodock 4. YouTube video tutorials were followed.

Retrieval and preparation of receptors

The 3D structures of target receptors PAF-R (PDB ID: 5ZKP), S1R (PDB ID: 5HK1) were retrieved from RCSB PDB in *.pdb format. Protein preparation wizard Autodock tools was used to remove water molecules accompanied by addition of polar hydrogen and Kollman charges. Then the atoms were assigned as AD4 type. The *.pdbqt format of the receptors were saved.

Retrieval and preparation of ligands

All the FDA approved drugs and phytochemicals 3D structures were obtained from NCBI PubChem in .sdf format followed by the conversion of *.sdf to *.pdbqt using Open Babel GUI. Further optimization was made by Autodock 4.2.6(Morris et al., 2014).

Blind docking by Autodock 4.2.6

Following the chemical alteration of the protein, a grid was set up so that the whole protein could be screened for potential binding sites by optimizing grid parameters as shown in the table 5. Then, a text file of the grid information was saved in the same folder, along with the protein in *.pdbqt format. The grid parameter file (*.gpf) also saved for the execution of Autogrid4.exe. GA runs were set to 10 and the population size was optimized to 150 in the search parameters which was saved in the Lamarckian format as docking parameter file (*dpf) to perform docking procedure.

Table 5: *Grid box parameters for BD*

Receptor	Size			Centre values			Spacing (Å)
	X	Y	Z	X	Y	Z	
5ZKP	70	70	126	39.172	-10.497	-16.018	0.800
5HK1	78	92	90	16.322	40.076	-31.560	0.575

Site-specific docking by Autodock 4.2.6

Receptor was separated from ligands for binding sites and non-standard residues such as waters, metals and heteroatoms were deleted in aims not to disrupt the docking. The missing atoms were repaired along with addition and spread of the Kollman charges. The grid box as per the table 6. Then the same procedures as BD was pursued.

Table 6: *Grid box parameters for SSD*

Receptor	Size			Centre values			Spacing (Å)
	X	Y	Z	X	Y	Z	
5ZKP	30	30	30	33.578	-4.452	7.541	0.513
5HK1	30	24	34	12.162	36.423	-34.778	0.375

Autodock vina and Argus lab

The above-mentioned steps from 2.2.3 and 2.2.4 were followed. Config.txt file was created as shown in the Figure 4 and vina.bat was generated and executed for all the ligands in a single step of execution.

```
receptor = 5zkp.pdbqt

center_x = 46.122
center_y = -19.753
center_z = -61.145

size_x = 30
size_y = 30
size_z = 30

num_modes = 50
energy_range = 4
exhaustiveness = 8
```

Figure 4: Config.txt file for 5ZKP

Analysis of docking parameters

Binding free energy, and inhibitory constant of docked complexes obtained from RMSD table which generated by the Autodock suite dlg file. The Vina output files was analyzed for binding affinity values.

Visualization of docking poses

BIOVIA DS

The PDB file of docked complex of the best docking pose was opened in BIOVIA DS.

UCSF Chimera

Phytochemical docked complexes were visualized as ribbon structure using UCSF Chimera. This was acquired by selecting 'publication' visualization.

Analysis of interactions

BIOVIA DS

The *.pdb file of the best docked complex was opened in the BIOVIA. Thereafter, the hydrogen interactions, unfavourable interactions, and hydrophobic interactions of the best docked pose in the 2D and 3D plane was visualized. The protein-ligand interactions such as HB, HPI (pi-pi, pi-psi, pi-alkyl) and the AAR in the active site were portrayed in 2D image (Butt et al., 2020).

LigPlot +

The *.pdb file of the best docked complex was opened in the LIGPLOT+ and the interactions between the ligand and the receptor with respect to the AAR that surrounds it was visualized.

Analysis of ADME properties

SwissADME web tool was used for initial screening of the phytochemicals through their canonical SMILES to determine drug likeliness, BBB permeability, GI absorption, and PAINS (Kalbhor et al., 2021).

Validation

Redocking

The validation of molecular docking was carried out by redocking natural ligand 9ER for the receptor: 5ZKP. For the receptor 5HK1, the natural ligand 61W was redocked for validation. The docking parameter had to be varied to generate the lowest free BE, a greater homogenous cluster distribution, and a lower RMSD value (< 2 Å). This validation was carried out using AutoDock and Vina parameters that was assisted by Python platform.

Ramachandran plot

Validation of receptors was performed by comparing the Ramachandran plot of docked complexes before and after docking, for the analysis of most favourable regions to validate the receptor using PROCHECK in SAVESv6.0 (Berry, Fielding and Gamieldien, 2015)

Super-imposition

Natural ligands were retrieved and superimposed with the redocked complex using PyMoL.

RESULTS

Autodock 4.2.6 and vina 1.2.6 results for 5ZKP

FDA-approved drugs

Table 7: *Results of docking of FDA approve drugs to target 5ZKP*

FDA drugs	BD BE (kcal/mol)	Ki (nM)	SSD BE (kcal/mol)	Ki (nM)	Vina BA (kcal/mol)
ABT-491_HCl	-7.38	3.92x 10^3	-11.78	2.33	-8.5
Azelastine	-9.47	114.25	-9.34	141.66	-9.7
Ketotifen	-7.53	3.02x 10^3	-8.61	486.83	-7.2
Rupatadine	-7.73	2.58x 10^3	-10.60	16.97	-8.0
Nilotinib	-8.02	1.33x 10^3	-10.76	12.96	-9.7

Based on BD, Azelastine (-9.47 kcal/mol) showed the higher BE and lowest Ki (114.25 nM), but ABT-491 hydrochloride exposed the highest BE (-11.78kcal/mol) and lowest Ki (2.33nM) in SSD against 5ZKP. However, nilotinib showed the highest BA(-9.7kcal/mol) in vina.

BD poses of FDA-approved drugs for 5ZKP

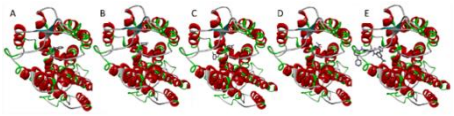

Figure 5: BD poses of FDA-approved drugs

Interactions of FDA-approved drugs for 5ZKP in BD

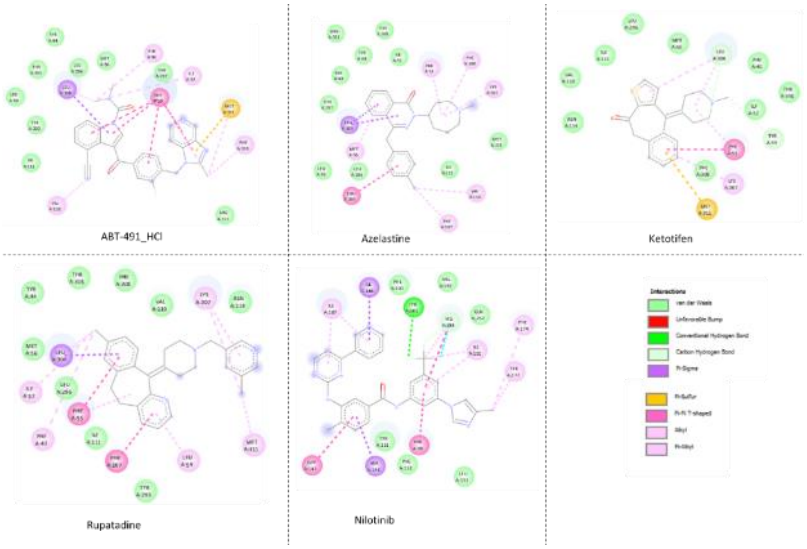

Figure 6: Interaction of FDA-approved drugs in BD

Table 8: *Interaction table of drugs from BD*

Phytochemical	HB	HPI
Azelastine	-	**PHE55**, PHE308, **LYS307**, VAL110, PHE107, TYR293, MET56, **LEU304**
ABT-491_HCl	-	PHE40, ILE52, **PHE55**, PHE308, VAL110, **LEU304**
Ketotifen	-	**PHE55**, **LYS307**
Rupatadine	-	**LYS307**, MET311, LEU59, PHE107, **PHE55**, PHE40, ILE52, **LEU304**
Nilotinib	TYR102	ILE186, ILE187, ILE191, PHE174, TYR177, PHE98, ALA148, GLY147

SSD poses of FDA-approved drugs for 5ZKP

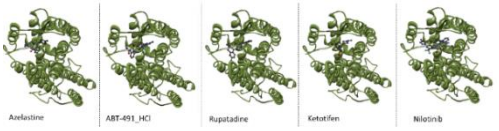

Figure 7: Docking poses of FDA approved drugs in SSD

Interactions of FDA-approved drugs for 5ZKP in SSD

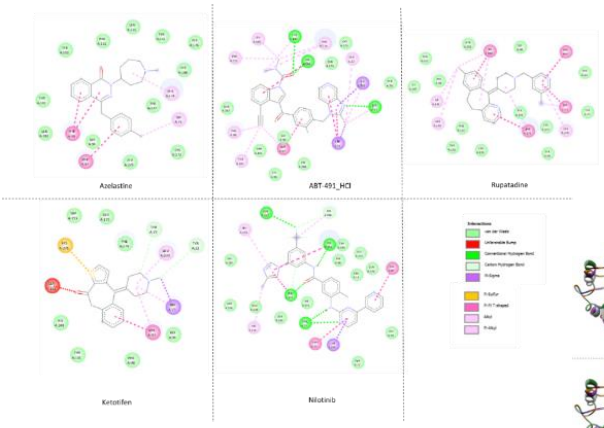

Table 9: *Interaction table of FDA approved drugs in SSD*

Phytochemical	HB	HPI
Azelastine	-	**PHE98, PHE97, TRP73, PHE174**
ABT-491_HCl	**TYR177**, HIS188, **TYR77**	LEU155, PHE152, **PHE98**, TYR102, **PHE97**, **TRP73**, **LEU279**, TYR22, **PHE174**
Ketotifen	-	**LEU279**, **PHE97**, **TRP73**
Rupatadine	-	HIS188, **PHE97**, **TRP73**, **PHE174**, VAL192, ILE191, **LEU279**
Nilotinib	**TYR177**, **TYR77**, GLN252, PHE174	LEU155, **PHE97**, **TRP73**, HIS176

Figure 8: SSD interactions of FDA approved drugs

vina docking poses of FDA-approved drugs for 5ZKP

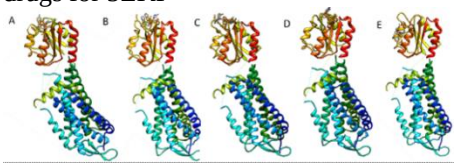

Figure 9: Docking poses of FDA-approved drugs in vina

Vina interactions

Phytochemicals for 5ZKP

Table 10: *vina interaction table for FDA-approved drugs in vina*

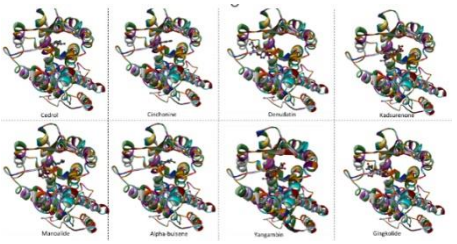

Figure 10: SSD poses of phytochemicals

Drug	HB	HPI
Azelastine	-	TRP1097, **TRP1059**
Nilotinib	THR1011, ASN1013, GLY1012, THR1010, ASP1094, THR1058, GLY1060, SER1057	TRP1097, **TRP1059**
ABT-491_HCl	-	**TRP1059**, TRP1097
Ketotifen	-	**TRP1059**
Rupatadine	-	ALA1106, TYR1099, ILE1064, LYS1110, LEU1066, ILE1071

In BD and SSD, Blazeispirol_X showed the higher BE (-9.89 and -11.54 kcal/mol) and lowest Ki in SSD (6.60 nM).

SSD poses of phytochemicals for 5ZKP

Phytochemical	5ZKP			
	Blind (kcal/mol)		Site (kcal/mol)	
	BE	Ki (μM)	BE	Ki (nM)
Ajmalimine	-6.45	18.72	-9.24	169.17
Cedrol	-7.36	4.03	-7.72	2190.0
Cinchonine	-7.23	4.99	-8.90	300.38
Gingkolide	-6.95	8.00	-7.95	1490.0
Kadsurenone	-7.07	6.54	-9.10	214.93
Kadsurin B	-6.44	18.89	-7.11	6100.0
Alpha-bulsene	-7.13	5.98	-7.59	2720.0
Alpinetin	-6.63	13.92	-7.37	3990.0
Andrographalide	-7.57	2.84	-10.99	8.83
Bakkenolide	-6.33	23.05	-7.34	4170.0
Blazeispirol X	-9.89	56.39	-11.76	6.60
Denudatin	-6.74	11.54	-7.91	1590.0
Kadsurin A	-7.04	6.89	-8.47	616.67
Epicatechin	-7.7	6.56	-9.76	70.50
Macluraxanthanone	-7.26	4.79	-8.96	271.94
Manoalide	-8.04	1.28	-9.73	73.94
Protopine	-8.10	1.15	-8.32	792.01
Puberulin	-9.7	77.33	-11.02	8.33
Scalaradial	-9.13	204.64	-10.29	28.47
Yangambin	-8.82	0.3415	-10.15	36.30

Figure 11: BD and SSD binding energy and inhibition constant

Interactions of phytochemicals for 5ZKP in SSD

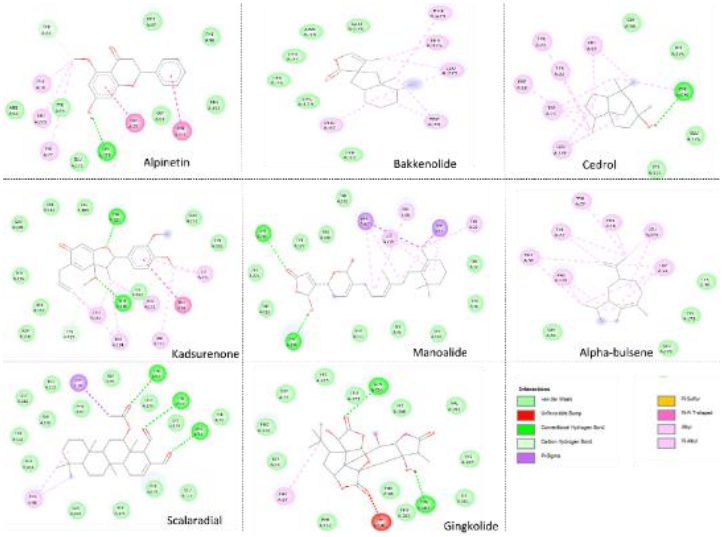

Figure12: SSD interactions of phytochemicals

Table 12: *SSD interaction table of phytochemicals*

Phytochemical	HB	HPI
Cedrol	PHE174	TYR77, **PHE97**, TYR22, PHE18, **TRP73**, **LEU279**
Kadsurenone	TYR151, HIS188	ILE191, PHE152, **PHE98**, VAL192, **PHE174**, LEU155
Alpinetin	CYS173	**PHE174**, **TRP73**, TYR77, **LEU279**, PHE18
Alpha-bulsene	-	TYR77, PHE18, **LEU279**, **TRP73**, **PHE174**, **PHE97**, TYR22
Manoalide	GLN252	**PHE97**, LEU279, **PHE98**, **TRP73**, TYR22
Bakkenolide	-	**PHE97**, **PHE174**, HIS275, **LEU279**, **TRP73**
Scalaradial	TYR22, TYR77, ARG14	**TRP73**, **PHE98**
Yangambin	TYR77	**PHE97**, **TRP73**, **LEU279**, PHE152, HIS188, **PHE98**, ILE191
Gingkolide	GLN252, TYR102	**PHE97**

Autodock 4.2.6 and vina 1.2.6 results for 5ZKP

FDA-Approved drugs for 5HK1

Table 13: Results of FDA-approved drugs for 5HK1

FDA drugs	BD BE (kcal/mol)	Ki (nM)	SSD BE (kcal/mol)	Ki (nM)	Vina BA (kcal/mol)
Risperidone	-11.4	6.80	-11.38	4.53	-12.9
Paliperidone	-9.23	172.04	-11.48	3.83	-12.6
Axitinib	-7.94	1.50	-10.42	22.94	-11.1
Atovaquone	-9.98	48.03	-11.23	5.90	-11.3
S1RA	-8.48	612.82	-8.95	274.62	-10.5

Risperidone showed the higher BE (-11.4 kcal/mol) and lowest Ki (6.8 nM) in BD and the highest BA (-12.9 kcal/mol) in vina but paliperidone exposed the highest BE (-11.48 kcal/mol) and lowest Ki (3.83nM) in SSD against 5HK1. However, nilotinib showed the highest BA(-9.7kcal/mol) in vina.

SSD poses of FDA-approved drugs for 5HK1

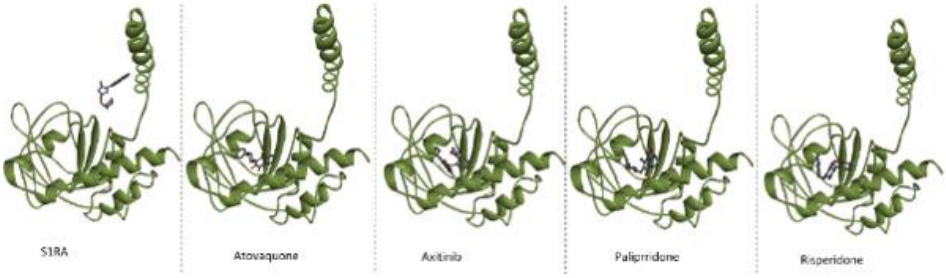

Figure 13: SSD poses of FDA-approved drugs

Interactions of FDA-approved drugs for 5HK1 in SSD

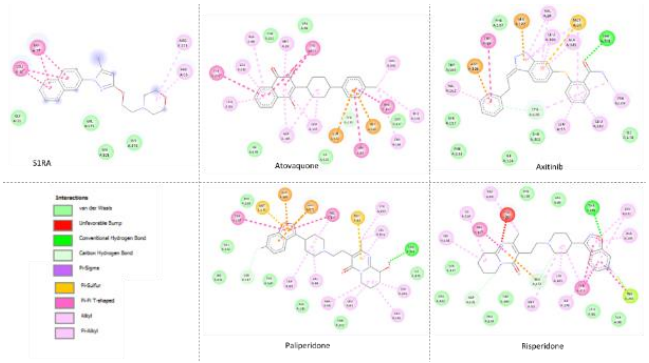

Figure 14: Interactions of FDA-approved drugs for 5HK1 in SSD

Table 13: *Interaction table of FDA approved drugs in SSD*

Drug	HB	HPI
Risperidone	**THR181**	**TRP89**, ILE124, **PHE107**, HIS154, LEU182, ALA185, **TYR103**, **LEU105**, ILE178, MET93
Paliperidone	**THR181**	TRP164, **PHE107**, **TRP89**, VAL84, ALA98, LEU95, LEU182, TYR206, **LEU105**, **TYR103**
Axitinib	**THR181**	VAL162, **TRP89**, VAL84, **LEU105**, ALA185, **TYR103**, LEU182, LEU95
Atovaquone	-	TYR206, LEU95, LEU182, ALA98, MET93, **TYR103**, ALA185, **LEU105**, **TRP89**, TRP164, PHE133, **PHE107**, VAL162, **TYR103**, MET93
S1RA	-	LEU30, TRP27, ARG175, PHE35

TRP89, PHE107, TYR103 & LEU105 were found as common AAR in 5HK1 from SSD

Vina docking poses of FDA-approved drugs for 5ZKP

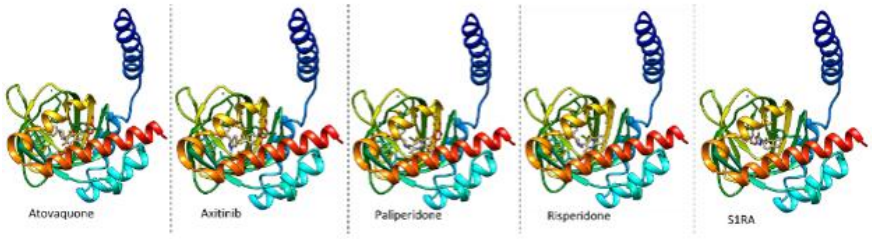

Figure 15: vina interactions for FDA approve drugs

Interactions of FDA-approved drugs in vina

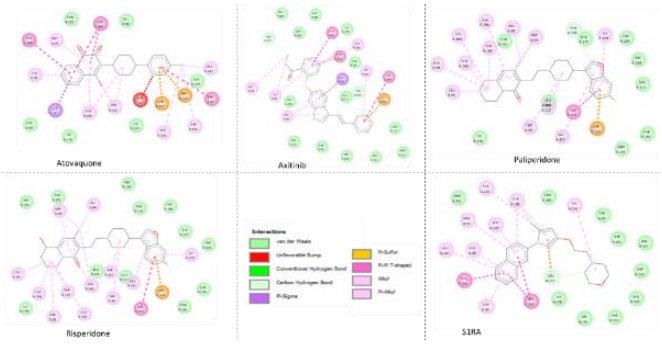

Table 14: *Interaction table for FDA-approved drugs from vina*

Drug	HB	HPI
Risperidone	-	ALA98, **LEU95**, **TYR206**, **TYR103**, **LEU182**, **ALA185**, VAL84, **MET93**, ILE124, HIS154, VAL162, TRP89, PHE107
Paliperidone	-	**MET93**, VAL84, ILE124, HIS154, VAL162, TRP89, PHE107, **ALA185**, **LEU182**, **TYR103**, **TYR206**, **LEU95**, ALA98
Axitinib	-	**MET93**, **LEU95**, VAL84, HIS154, ILE124, **ALA185**, **TYR103**, **LEU182**, **TYR206**
Atovaquone	-	**TYR206**, **LEU95**, **MET93**, **LEU182**, **ALA185**, LEU105, PHE133, TRP164, TRP89, VAL162, **TYR103**
S1RA	-	TYR120, **ALA185**, ILE124, **TYR103**, **LEU95**, **TYR206**, **LEU182**, ALA98, **MET93**, LEU105

LEU95, TYR206, TYR103, LEU182, ALA185, MET93 were identified as common AAR in 5HK1 from vina

Phytochemicals for 5HK1

Table 15: *BE and Ki of phytochemicals in BD and SSD for 5HK1*

Phytochemical	5HK1			
	Blind (kcal/mol)		Site (kcal/mol)	
	BE	Ki (μM)	BE	Ki (nM)
Ajmalimine	-6.57	15.18	-7.68	2360.0
Cedrol	-7.55	2.91	-7.5	3200.0
Cinchonine	-7.66	2.41	-9.09	217.87
Gingkolide	-5.72	64.60	-6.86	9350.0
Kadsurenone	-6.2	28.63	-8.25	896.79
Kadsurin B	-5.51	90.68	-8.79	358.27
Alpha-bulsene	-7.72	4.72	-7.45	3480.0
Alpinetin	-7.27	4.72	-7.26	4770.0
Andrographalide	-7.68	2.33	-9.93	52.20
Bakkenolide	-7.30	4.48	-7.86	1740.0
Blazeispirol X	-8.57	0.5240	-8.48	606.45
Denudatin	-8.52	0.5670	-8.88	308.57
Kadsurin A	-6.74	11.52	-9.12	205.93
Epicatechin	-8.23	0.9314	-9.65	84.30
Macluraxanthanone	-4.78	314.05	-7.79	1970.0
Manoalide	-9.6	0.1163	-10.18	34.35
Protopine	-7.54	2.96	-8.19	998.18
Puberulin	-7.99	1.39	-9.96	50.30
Scalaradial	-7.88	1.68	-8.76	376.34
Yangambin	-7.8	1.67	-9.59	93.89

SSD poses of phytochemicals for 5HK1

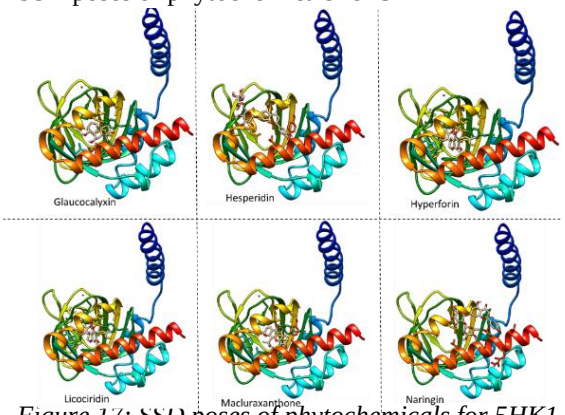

Figure 17: SSD poses of phytochemicals for 5HK1 in chimera

SSD interactions of phytochemicals for 5HK1

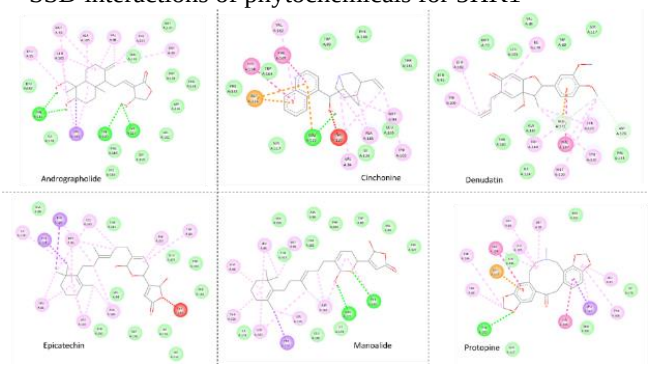

Table 16: *SSD interaction table of phytochemicals for 5HK1*

Phytochemical	HB	HPI
Protopine	TYR120	**MET93**, VAL84, **LEU105**, **PHE107**, TRP164, TRP89, **TYR103**, LEU182, TYR206, **LEU95**
Manoalide	**GLU172**, TYR120	**LEU95**, **MET93**, ALA98, TYR206, LEU182, **LEU105**, ALA185
Epicatechin	-	ILE178, **TYR103**, TYR206, **MET93**, **LEU105**, **LEU95**, LEU182, ALA185, **PHE107**, TRP89
Denudatin	-	LEU182, ILE178, TYR206, TRP164, **PHE107**, MET170, TYR120, **TYR103**
Cinchonine	**GLU172**	VAL162, HIS154, **PHE107**, VAL84, ALA185, **TYR103**, **MET93**
Andrographolide	THR181, TYR120, SER117	LEU95, **LEU105**, **MET93**, ALA185, VAL, **PHE107**, TRP89, **TYR103**

Figure 18: SSD interactions of phytochemicals for 5HK1

With respect to HB, GLU172 was identified as a common AAR and MET93, LEU105, PHE107, TYR103 and LEU95 were identified as common AAR with respect to HPI.

Table 17: *Autodock vina BA and ADME analysis for phytochemicals for 5ZKP and 5HK1*
Autodock vina results and ADME analysis for phytochemicals for 5ZKP and 5HK1

Phytochemical	Binding affinity (kcal/mol) 5ZKP	Binding affinity (kcal/mol) 5HK1	ADMET properties			
			Lipinski's Rule	BBB	GI abso.	PAINS
Ajmalimine	-10.8	-6.1		X	High	X
Alpinetin	-9.4	-9.2			High	X
Cinchonine	-9.6	-9.5			High	X
Curcurmin	-9.4	-9.6		X	High	X
Denudatin B	-9.0	-9.3			High	X
Epicatechin	-11.5	-10.6		X	High	1 alert
Gingkolide B	-10.7	-5.3		X	Low	X
Glaucocalyxin A	-9.9	-8.9			High	X
Gossypol	-10.8	-5.6	X	X	Low	1 alert
Herquline B	-9.4	-5.4			High	X
Hesperidin	-10.5	-6.0	X	X	Low	X
Hyperforin	-10.9	-4.8	X	X	Low	X
Kadsurenone	-9.1	-9.2			High	X
Kadsurin A	-9.5	-8.6			High	X
Kadsurin B	-9.4	-9.0			Low	X
Licoricidin	-10.0	-10.9		X	High	X
Liriodenine	-10.1	-8.8			High	X
Macluraxanthone	-11.1	-7.6		X	High	1 alert
Naringin	-10.6	-5.6	X	X	Low	X
Neferine	-10.9	-6.2		X	High	X
Nimolicinol	-9.5	-5.9		X	High	X
Pinusolide	-9.5	-9.1			High	X
Prehispanolone	-9.9	-6.7			High	X
Proanthocyanidin	-9.6	-6.1	X	X	Low	X
Protopine	-10.7	-9.6			High	X

Puberulin	-11.7	-6.3			High	X
Yangambin	-9.7	-7.4		X	High	X
Blazeispirol X	-12.1	-7.0		X	High	X
Berberine	-9.4	-10.5			High	X
Berberastine	-9.5	-9.3			High	X
Manoalide	-11.5	-10.6		X	High	X
Phomactin A	-9.9	-5.3			High	X
Phillygenin	-9.7	-10.3			High	X
Rubraxanthone	-10.3	-9.9		X	High	X
Silibinin	-11.0	-9.8		X	Low	X

Blazeispirol X, Puberulin and Epicatechin showed the higher BE and relatively significant lower Ki for both BD and SSD with the BBB permeability, an essential feature of a drug candidate for IS against 5ZKP. GI absorption including caco-2, which is considered as gold standard method for orally administered drugs to assess active and passive transport and absorption is also positively high in most of the phytochemicals. Pan-assay interference compounds (PAINS) are uninhibited molecules which lead to false-positive problems. Therefore, only 3 compounds have PAINS among the series of phytochemicals as depicted in Table 21. For 5HK1, Licoridicin, epicatechin, and manoalide showed significantly higher BA (-10.9, -10.6 and -10.6 kcal/mol respectively) but the BBB permeability is unavailable for them and epicatechin has 1 PAINS alert. AAR found in the binding site of 5ZKP is shown in the Table 22 while the bold texts depict the common AAR.

Docking poses of vina docking for 5ZKP

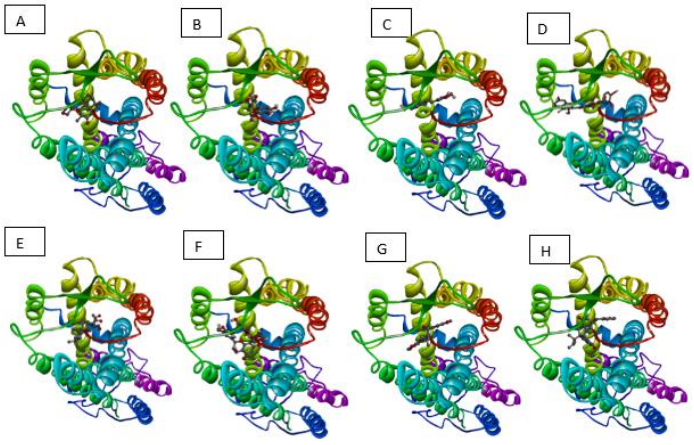

Figure 19: Best DP of (A) Prehispanolone (B) Proanthocyanidin (C) Protopine (D) Puberulin (E) Quercetin (F) Resveratol (G) Silibinin (H) Yangambin in vina for 5ZKP

Interactions of phytochemicals for 5ZKP

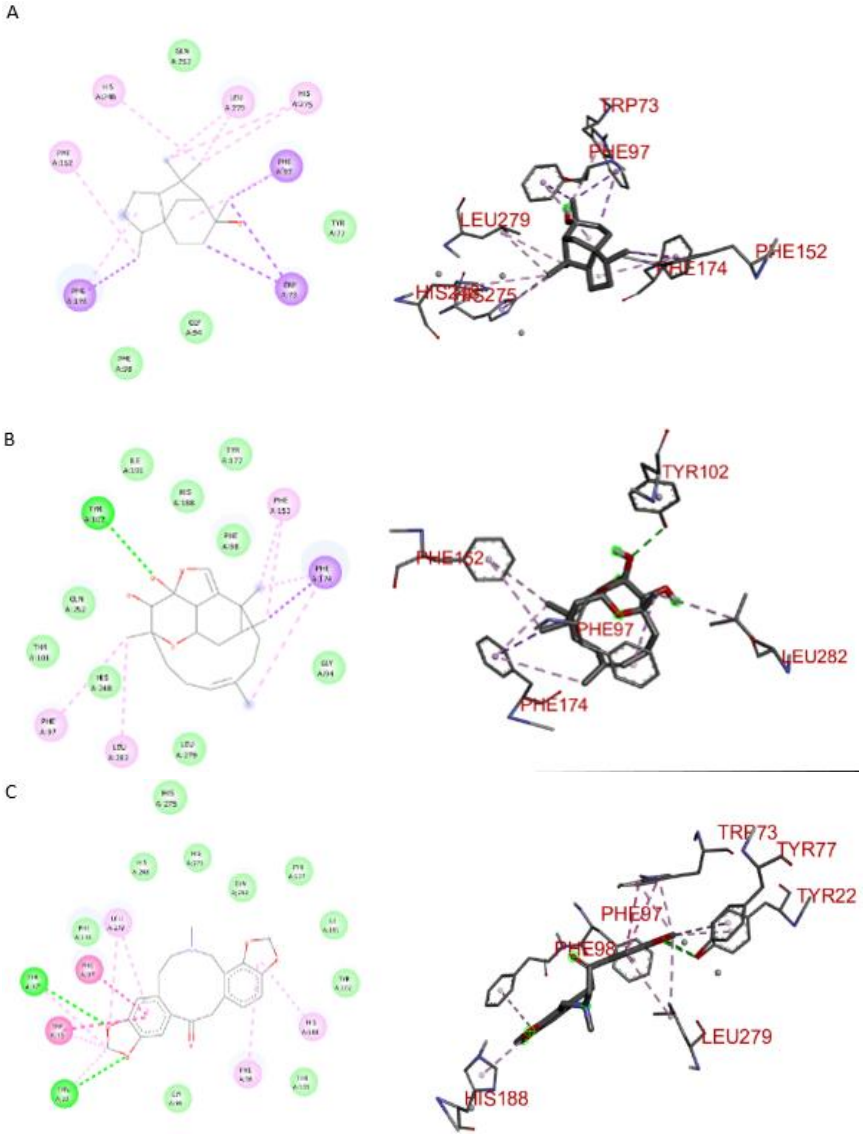

Figure 20: 2D images of the interactions of (A) Epicatechin (B) Manoalide (C) Protopine in vina for 5ZKP

Table 18: *Interactions table of 5ZKP in vina*

Ligands	HB	HPI
Blazeispirol x	TYR22, TYR77	PHE174, HIS188, HIS275, HIS248, HIS249, LEU282, TYR102, PHE98, PHE97, TRP73, LEU279
Protopine	TYR77, TYR22	LEU279, PHE97, TRP73, PHE98, HIS188
Liriodenine	TYR77	TRP73, PHE97, LEU279, HIS275
Glaucocalyxin A	TYR77, PHE174	-
Yangambin	TYR22, TYR77, ARG14	HIS249, HIS248, PHE98, PHE97, TRP73, PHE174, HIS275
Chinchonine	-	PHE97, LEU279, TRP73, HIS248, TYR102, PHE98
Berberastine	-	TRP73, LEU279, PHE97, VAL192, PHE98, ILE191
Kadsurin A	-	TYR77, TYR22, TRP73, LEU279, HIS275, HIS248, GLN252
Alpinetin	TYR102	PHE98, PHE152, PH 97, LEU279, TRP73
Andrographolide	TYR102	PHE98, PHE97
Apigenin	GLN252, TYR177	LEU279, PHE174, TRP73, PHE97
Bakkenolide A	-	HIS248, TRP73, LEU279, PHE97
Curcurmin	TYR77	TRP73, LEU279, PHE97, PHE174
Herquilin B	-	-
Lutelion	TYR177, GLN252, TYR77	LEU279, TRP73, PHE97, PHE174
Paliperidone	TYR151	PHE152, HIS188, PHE98, PHE174, LEU155, TYR177, PHE97, TRP73, LEU 79
Piperenone	TYR77	LEU279, TRP73, PHE18, PHE174, PHE97, TYR102, LEU282
Quercetin	CYS173, TYR77	LEU279, PHE97, GLU175
Resveratol	TYR22	TRP73, PHE97, LEU279, PHE174

Epicatechin	TYR177, HIS188	PHE152, PHE174, LEU279, HIS275, TRP73, PHE97
Prehispanolone	HIS188	TYR177, PHE174, LEU279, PHE97
Kadsurin b	-	ILE191, HIS188, LEU279, HIS248, HIS275, TRP73, PHE97
Manoalide	TYR177, HIS188, TYR151	PHE174, PHE152, HIS275, LEU279
Puberulin	-	TRP73, PHE97, LEU279, PHE98, HIS188, ILE191
Phomactin A	TYR102	PHE152, PHE174, LEU282, PHE97
Macluraxanthanone	ILE187, GLN252	HIS188, ILE191, PHE98, PHE152, TYR177, LEU279, TRP73, PHE97, PHE174
Silibinin	TYR151, ARG14	PHE174, TYR177, VAL184, LEU155, VAL182, HIS275, TRP 255

Interaction s of phytochemicals in vina for 5HK1

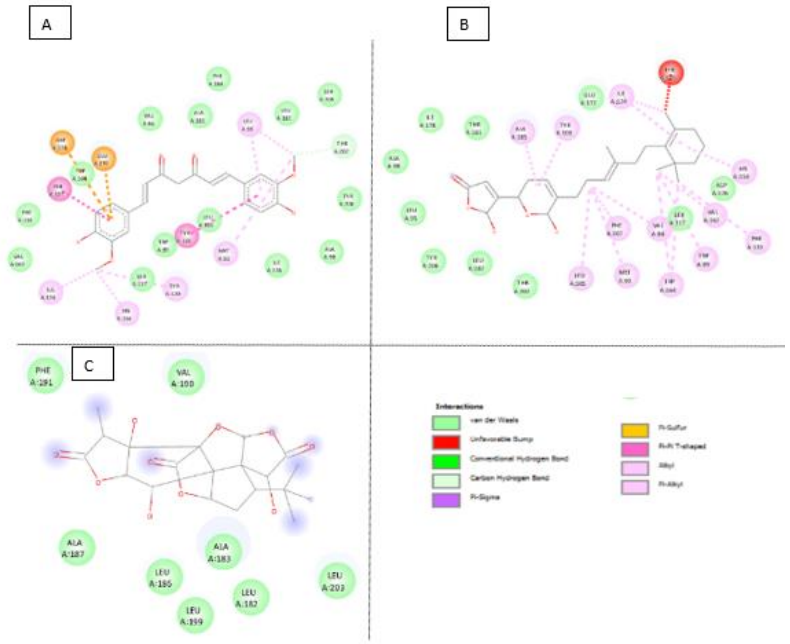

Figure 21: Interactions of (A) Licoricidin (B) Macluraxanthone (C) Naringin

Table 19: *Interactions table of phytochemicals for 5Hk1*

Ligands	HB	HPI
Naringin	LEU210	-
Manoalide	-	ALA185, LEU105, TYR103, MET93, PHE107, ILE124, HIS154, VAL162, PHE133, TRP89, VAL84, TRP164
Macluraxanthone	THR181, THR202	LEU95, LEU182, VAL84, LEU105, ALA185, TRP89, PHE184, PHE107
Licociridin	-	TRP89, PHE107, LEU105, ALA185, LEU95, ILE178, LEU182, TYR103, VAL162, VAL84, PHE133, VAL152, HIS154
Hyperforin	-	LEU182, ALA183, LEU203, LEU186, LEU199, ALA187, PHE191
Hesperidin	LEU203	
Glaucocalyxin	-	TYR103, TYR120, ALA185, TRP89
Gingkolide	-	-
Epicatechin	-	ALA185, TYR103, ILE124, HIS154, VAL162, PHE133, TRP89, TRP164, VAL84, PHE107, LEU105, MET93
Curcumin	-	PHE107, LEU95, MET93, TYR103, TYR120, HIS154, ILE124

The docked BE (kcal/mol) of ligands with different software are presented in Table 24.

3.5 Comparison of BE among 4 software

Table 20: *Docked results in different software*

Phytochemical	AD4	Vina	Chimera	ArgusLab
Blazeispirol X	-11.76	-12.1	-11.8	-17.33
Epicatechin	-9.76	-11.5	-11.9	-17.43
Puberulin	-11.02	-11.7	-9.4	-16.99

Based on all the docking techniques, blazeispirol X showed higher BE.

Validation

Redocking

Table 21: *Redocking values and RMSD*

Natural ligand	AD4 SSD		Vina	
	BE (kcal/mol)	RMSD (Å)	BA (kcal/mol)	RMSD (Å)
9ER (5ZKP)	-10.22	0.652	-10.7	0.382
61W (5HK1)	-9.3	0.928	-10.1	0.354

The RMSD value of Vina (0.382Å and 0.354Å) was better than AD4 (0.652Å and 0.928 Å) as it was surveyed to be the lowest for 5ZKP and 5HK1 respectively. Since the RMSD value of superimposing is < 2.00 Å, it is validated the orientation and the conformations of the ligands are appropriate (Al-Khodairy et al., 2013).

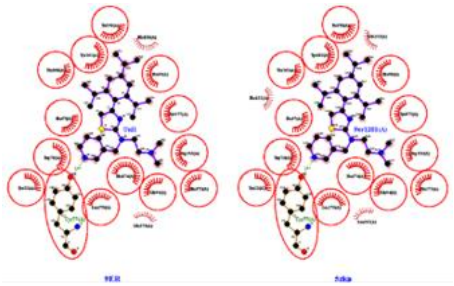

Figure 22: Ligplot+ for redocked complex

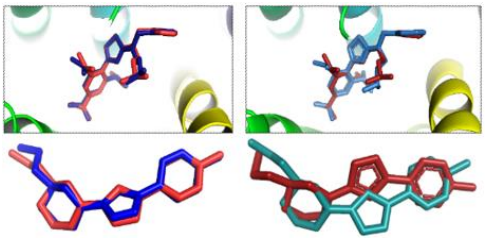

Figure 23: Superimposed images of (A) 9ER in vina (B) 9ER in AD4 (C) 61W in AD4 (D) 61W in vina

Ramachandran plot analysis

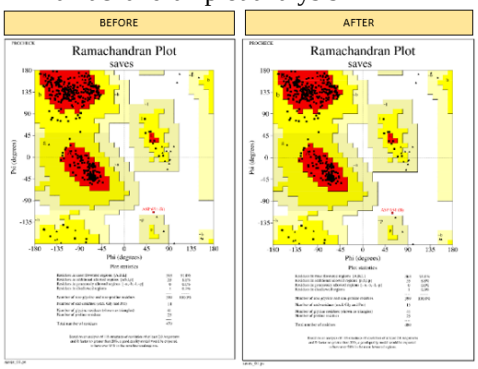

Figure 24: Ramachandran plots before and after docking

The Ramachandran analysis for 5ZKP exemplified that, 363 (91.0%) residues are in most favoured region, 35 (8.8%) are in additionally allowed region and no residues in generously allowed regions. There was 1 residue in outlier region, which can be disregarded.

In Ramachandran analysis for 5HK1, 94.1% of residues are in most favoured region and 5.9% is in additional allowed region while no residues fall under generously allowed or disallowed region.

DISCUSSION

Computational approaches are of prodigious importance as they assist in detecting and developing novel capable compounds, particularly by molecular docking methods in pharmaceutical research. Several appraisals have applied docking methodology to discover probable novel compounds against diverse diseases. Platelet-activating factor receptor and sigma-1-receptor (5ZKP and 5HK1) have become crucial therapeutic targets for IS. As 5ZKP has only A chain, the step for the deletion of unwanted chains was skipped. However, B and C chains of 5HK1 were deleted as the binding site is in the A chain and to reduce the period for protein preparation and docking. Water molecules and heteroatoms were deleted with the aim not to interrupt the binding site. Kollman charges, calculated from electrostatic potential, were added to 5ZKP and 5HK1, to calculate the net atomic charges and missing atoms are repaired to optimize the physiological protein (Geidl et al., 2015).

To identify the HB interactions, the polar hydrogen atoms were added.

BD is beneficial if the binding pocket of the receptor remains unknown. The highest grid point, 126 is usually utilized in BD to cover the entire receptor, although the accuracy error is probably related to short intermolecular distances of dispersions and HB where the spacing value ranges from 0.375Å to 1Å for BD and SSD. With relevant to the binding pocket, SSD encloses only the interactive site by a specific grid points value. According to Darwin's theory of evolution, a genetic algorithm runs (GA) is a built-in program in AD4 which presumes the best docking pose and demarcate the quality and reliability of the docking outputs (Ordog and Grolmusz, 2008). Thus LGA, which processes ligands with higher degrees of freedom with 50 GA runs were executed (Population size: 300) for increased search efficiency and to attain the maximum possible docking poses to finalize the most precise and appropriate conformation of the ligand.

Conversely, Vina utilizes a gradient optimization algorithm and several CPUs with a default number of iterations at 10 which lowers the period of docking and escalate the output of the execution. 'Monte-Carlo iterated local search method' is used in vina which involves iterations of sampling, scoring and optimization. Scoring function calculates and estimate BE which defines the total of the ligand-receptor (intermolecular energy) and the ligand-ligand (intramolecular energy). Furthermore, the conformation is optimized with a Broyden-FletcherGoldfarb-Shanno (BFGS) method (Fletcher, 2013) that considers the gradients of the scoring function. Ligands are directed by these gradients to achieve a better conformation with a lower docking score. Despite halogen and guanidine-arginine interactions regulate the protein-ligand interactions significantly, scoring function cannot formulate precise BEs/BAs as those interactions are not deliberated as it is considered as a major limitation (Yang et al., 2015 and Ren et al., 2014).

Predominantly, selection of the best performing ligands against 5ZKP and 5HK1 is based on the BE and BA accompanied by ADME properties of phytochemicals. (Yang et al., 2015 and Ren et al., 2014). Moreover, common AAR with respect to HB and HPI were identified attested by previous studies, and newer interactions were noted from the current study for further analysis. Ligand specificity is decided corresponding to the numbers of HBs and HPI found in the binding site. Thus, higher numbers of interacting AAR show proficient binding of ligand to the target protein (de Freitas and Schapira, 2017). Table 26 depicts the comparison of this study and the previous study (El Mchichi et al., 2021). AAR which are common in both the studies are in bold.

Table 22: *Comparison of results with previous study*

Phytochemical	**Study value** kcal/mol	**previous value** kcal/mol	**This study AAR for 5ZKP**	**Previously found AAR For 5ZKP** (*El Mchichi et al.*, 2021)
Cedrol	-8.1	-8.1	**PHE174, TRP73, PHE97**, HIS275, LEU279, HIS248, PHE152	**PHE174, TRP73, PHE97**
Kadsurenone	-9.1	-8.8	PHE98, PHE174, LEU155, PHE152, ILE191, VAL192 (HB- HIS188, **TYR102**, TYR151)	LEU279, PHE18, TRP73, PHE97, HIS188 (HB- TYR77, **TYR102**

In this study, the BA of Kadsurenone is higher and Kadsurenone-5ZKP showed higher HB and HPI than by El Mchichi et al., 2021. Cedrol-5ZKP has the similar BA as the previous study with additional hydrophobic bonds.

As attested by Battista et al., 2021, some FDA-approved drugs BEs for 5HK1 showed lower value than this current study as shown in the Table 27.

Table 23: *FDA-drugs comparisons*

Drug	Previous study value (Battista et al., 2021) kcal/mol	This study values kcal/mol
Risperidone	-12.6	-12.9
Paliperidone	-12.2	-12.6

Corresponding to the results, conclusion can be drawn as ABT-491_HCl is a best-fit FDA-approved drug to target 5ZKP from SSD. Hence, nilotinib can be administered as it has more HBs, and BA is also high in vina. To target 5HK1, risperidone is an effective drug based on AD4 and vina. Blazeispirol X shows tendency to target 5ZKP in all the techniques and manoalide is identified to treat IS via 5HK1. As the common AAR of 5ZKP, with respect to HB, TYR77 was found and PHE97, PHE174 TRP73, and LEU279 were identified with respect to HPI. MET93, ALA185, LEU182, TYR103, TYR206, and LEU495 were the common AAR in 5HK1. Based on the results, performance of vina is well defined, and these phytochemicals are more prone to target 5ZKP than 5HK1.

Future work

The enigma of this docking study is the receptor is being rigid which may affect the scoring function. Although the protein is rigid in the study, it also naturally has various conformation. This challenge can be overcome by in silico MD including flexible docking or molecular dynamic simulation. MD trajectories which involve PCA for a specific site of the receptors, can be followed further. Network pharmacology including PPI and pivotal gene analysis can be performed based on this research to validate the neuroprotective effects and mechanism of neuroprotection and pathophysiology of phytochemicals. Experimental, and computational validation techniques such as GO analysis, KEGG pathway enrichment using DAVID are beneficial to continue the study further (Dong et al., 2021). Cell survival assay, qRT-PCR and western blotting can be followed to assess in vitro culture models of IS. QASR study can be done for the set of phytochemicals. Best QSAR analysis can be performed to assess IGC50 for phytochemicals. In future, puberulin can be extracted from Agathosma martiana through atmospheric pressure ionization (API) LC-MS techniques which can utilize either APCI or ESI. To evaporate the solvent, the eluant from the HPLC column is sprayed through a co-axial capillary with a heated gas in APCI (Donald et al., 2021). PASS prediction also will be performed for selected phytochemicals. Further, the advanced sophisticated docking software such as schrodinger GLIDE can be utilized to execute and obtain more productive outputs. Estimation of an entire methodical exploration of the docked ligands' conformational, orientational, and positional space is carried out by GLIDE (Friesner et al., 2004).

Acknowledgment

This research was supported by school of science, Business Management School (BMS) affiliated with Northumbria university. I thank the principal supervisor Ms. Heshani Mudalige from BMS who provided insight and expertise that greatly assisted the research. Many special thanks

to my adviser and supervisor Mr Ominda Perera, who read my draft and helped make some sense of the confusions. I am sincerely grateful to Ms Heshani Mudalige for offering immense guidance and support. I would like to thank my colleagues for their generous guidance throughout the project. Special thanks to Dr.Mathi for her guidance and motivation.

REFERENCES

Agnihotry, S., Pathak, R., Singh, D., Tiwari, A. and Hussain, I. (2022) 'Protein structure prediction', Bioinformatics, pp. 177-188 [Online]. DOI:10.1016/b978-0-323-89775-4.00023-7 (Accessed: 19th July 2022).

Ahamad and Tanveer (2021) 'Workflow docking with Autodock 4:', A Beginner's Guide [Online]. DOI: 10.13140/RG.2.2.11230.77122 (Accessed: 19th July 2022).

Al-Khodairy, F. M., Khan, M. K. A., Kunhi, M., Pulicat, M. S., Akhtar, S. and Arif, J. M. (2013) 'In silico prediction of mechanism of erysolin-induced apoptosis in human breast cancer cell lines', American Journal of Bioinformatics Research, 3(3), pp. 62-71 ResearchGate [Online]. Available at: https://citeseerx.ist.psu.edu/viewdoc/download?doi=10.1.1.1060.9122&rep=rep1&type=pdf (Accessed: 20 April 2022).

Battista, T., Pascarella, G., Staid, D., Colotti, G., Rosati, J., Fiorillo, A., Casamassa, A., Vescovi, A., Giabbai, B., Semrau, M., Fanelli, S., Storici, P., Squitieri, F., Morea, V. and Ilari, A. (2021) 'Known drugs identified by structure-based virtual screening are able to bind sigma-1 receptor and increase growth of huntington disease patient-derived cells', International Journal of Molecular Sciences, 22(3), p.1293 [Online]. DOI: 10.3390/ijms22031293 (Accessed: 1 August 2022).

Bazan, N., Khoutorova, L., Alvarez-Builla, J. and Belayev, L. (2015) 'Abstract W P251: novel platelet-activating factor receptor antagonists attenuate brain injury after experimental stroke', Stroke, 46(1) [Online]. DOI: 10.1161/str.46.suppl_1.wp251. (Accessed: 19 July 2022).

Berry, M., Fielding, B. C. and Gamieldien, J. (2015) 'Potential Broad-Spectrum Inhibitors of the Coronavirus 3CLpro: A Virtual Screening and Structure-Based Drug Design Study', Bioinformatics and Computational Biology of Viruses, 7 (12), pp. 6642-6660, Molecular Diversity Preservation International [Online]. DOI: https://doi.org/10.3390/v7122963 (Accessed: 20 April 2022).

Brahmachari, G. (2017) 'Andrographolide', Discovery and Development of Antidiabetic Agents from Natural Products, pp.1-27 [Online]. DOI: 10.1016/b978-0-12-809450-1.00001-6 (Accessed: 1 August 2022).

Bridi, H., Meirelles, G., Bordignon, S., Rates, S. and von Poser, G. (2017) 'Denudatin A, a Dimeric Acylphloroglucinol from Hypericum denudatum Presents an Antinociceptive Effect in Mice', Planta Medica, 83(17), pp.1329-1334 [Online]. DOI: 10.1055/s-0043-109567 (Accessed: 1 August 2022).

Butt, S.S., Badshah, Y., Shabbir, M. and Rafiq, M. (2020) 'Molecular docking using Chimera and Autodock vina software for non-bioinformaticians', JMIR bioinformatics and biotechnology, 1(1), p.14232 [Online]. DOI: 10.2196/14232 (Accessed: 19 July 2022).

Cao, C., Zhao, Q., Zhang, X., and Wu, B. (2018) 'Crystal structure of the human platelet-activating factor receptor in complex with SR 27417', [Online]. DOI: 10.1038/s41594-018-0068-y (Accessed: 25 March 2022).

Chauhan, G. and Debette, S. (2016) 'Genetic Risk Factors for Ischemic and Hemorrhagic Stroke', Current Cardiology Reports, 18(12).

[Online]. DOI:10.1007/s11886-016-0804-z (Accessed: 19 July 2022).

De Freitas, R. F. and Schapira, M. (2017) 'A Systematic Analysis of Atomic Protein–Ligand Interactions in the PDB', MedChemComm, 8(10), pp. 1970-1981 National Center for Biotechnology Information [Online]. DOI: 10.1039%2Fc7md00381a (Accessed: 15 March 2022).

Donald, G., de Carvalho, P., Fernandes, P. and Boylan, F. (2021) 'Antinociceptive activity of puberulin and choisyine from ethanol extract of Choisya ternata Kunth var. Sundance', Biomedicine & Pharmacotherapy [Online]. DOI: 10.1016/j.biopha.2021.111926 (Accessed: 1 August 2022).

Dong, R., Huang, R., Shi, X., Xu, Z. and Mang, J. (2021) 'Exploration of the mechanism of luteolin against ischemic stroke based on network pharmacology, molecular docking and experimental verification', Bioengineered, 12(2), pp.12274-12293 [Online]. DOI: 10.1080/21655979.2021.2006966 (Accessed: 1 August 2022).

Donkor, E. (2018) 'Stroke in the21stCentury: A Snapshot of the Burden, Epidemiology, and Quality of Life', Stroke Research and Treatment, pp.1-10. [Online]. DOI:10.1155/2018/3238165 (Accessed: 19 July 2022).

Durukan, A. and Tatlisumak, T. (2007) 'Acute ischemic stroke: Overview of major experimental rodent models, pathophysiology, and therapy of focal cerebral ischemia', Pharmacology Biochemistry and Behavior, 87(1), pp.179-197. [Online]. DOI:10.1016/j.pbb.2007.04.015 (Accessed: 19 July 2022].

El-Hachem, N., Haibe-Kains, B., Khalil, A., Kobeissy, F.H. and Nemer, G (2017) 'AutoDock and AutoDockTools for Protein-Ligand Docking: Beta-Site Amyloid Precursor Protein Cleaving Enzyme 1(BACE1) as a Case Study', pp. 391-403 [Online]. DOI:10.1007/978-1-4939-6952-4_20 (Accessed: 1 August 2022).

Elmchichi, L., Bouachrine, M., El Aissouq, A., Belhassan, M., Zaki, H., Ouammou, A., and Lakhlifi, T. (2021) 'Molecular Docking, Drug likeness Studies and ADMET prediction of Flavonoids as Platelet-Activating Factor (PAF) Receptor Binding', Chemical Review and Letters, 4(3) pp.145-152 [Online]. DOI: 10.22034/crl.2021.262806.109 (Accessed: 1 August 2022).

Friesner, R., Banks, J., Murphy, R., Halgren, T., Klicic, J., Mainz, D., Repasky, M., Knoll, E., Shelley, M., Perry, J., Shaw, D., Francis, P. and Shenkin, P. (2004) 'Glide: A New Approach for Rapid, Accurate Docking and Scoring. 1. Method and Assessment of Docking Accuracy', Journal of Medicinal Chemistry, 47(7), pp.1739-1749 [Online]. DOI: 10.1021/jm0306430 (Accessed: 1 August 2022).

Hernández-Santoyo, A., Tenorio-Barajas, A. Y., VictorAltuzar, V., Vivanco-Cid, H. and Mendoza-Barrera, C. (2013) 'Protein-Protein and Protein-Ligand Docking. In (Ed.), Protein Engineering - Technology and Application', IntechOpen [Online]. DOI: 10.5772/56376 (Accessed: 19 July 2022).

Huang, S. Y. and Zou, X. (2010) 'Advances and challenges in protein-ligand docking. International Journal of Molecular Sciences', 11(8), pp. 3016-3034. [Online]. DOI:10.3390/ijms11083016 (Accessed: 19 July 2022).

Huang, S., Lin, L., Wu, Y. and Tsai, T. (2009) 'Pharmacokinetics of kadsurenone and its interaction with cyclosporin A in rats using a combined HPLC and microdialysis system', Journal of Chromatography, 877(3), pp.247-252 [Online]. DOI: 10.1016/j.jchromb.2008.12.019 (Accessed: 19 July 2022).

Kalbhor, M. S., Bhowmick, S., Alanazi, A. M., Patil, P. C., and Islam, M. A. (2021) 'Multi-step Molecular Docking and Dynamics Simulation-based

Screening of Large Antiviral Specific Chemical Libraries for Identification of Nipah Virus Glycoprotein Inhibitors', Biophysical Chemistry, ScienceDirect [Online]. DOI: 10.1016/j.bpc.2020.106537 (Accessed: 20 April 2022).

Katan, M. and Luft, A. (2018) 'Global Burden of Stroke', Seminars in Neurology, 38 (2), pp.208-211 [Online]. DOI: 10.1055/s-0038-1649503 (Accessed: 1 August 2022).

Kuriakose, D. and Xiao, Z. (2020) Pathophysiology and Treatment of Stroke: Present Status and Future Perspectives. International journal of molecular sciences, 21(20), 7609 [Online]. DOI:10.3390/ijms21207609 (Accessed 19th July 2022).

Laskowski, R. and Swindells, M. B. (2011) 'LigPlot+: Multiple Ligand-Protein Interaction Diagrams for Drug Discovery, Journal of Chemical Information and Modelling, 51(10), pp. 2778-2786. American Chemical Society Publications [Online]. DOI: 10.1021/ci200227u (Accessed: 20 April 2022).

Liaw, N. and Liebeskind, D. (2020) 'Emerging therapies in acute ischemic stroke'. F1000Research, 9 [Online]. DOI: 10.12688/f1000research.21100.1 [Accessed 19th July 2022].

Martins, J., Coelho, J., Tadini, M., de Souza, R., Figueiredo, S., Fonseca, M., de Albuquerque, N., Lopes, N., Berretta, A., Marquele-Oliveira, F. and de Oliveira, A. (2020) 'Yangambin and Epi-yangambin Isomers: New Purification Method from Ocotea fasciculata and First Cytotoxic Aspects Focusing on In Vivo Safety', Planta Medica, 86 (06), pp.415-424 [Online]. DOI: 10.1055/a-1118-3828 [Accessed 1st August 2022].

Meng, X., Zhang, H., Mezei, M. and Cui, M. (2011) 'Molecular Docking: A Powerful Approach for Structure-Based Drug Discovery', Current Computer Aided-Drug Design, 7 (2), pp.146-157 [Online]. DOI: 10.2174/157340911795677602 (Accessed: 1 August 2022).

Moon, S., Chang, M.-S., Koh, S.-H., and Choi, Y. K. (2021) Repair Mechanisms of the Neurovascular Unit after Ischemic Stroke with a Focus on Vegf. Int. J. Mol. Sci. 22, 8543 [Online]. DOI:10.3390/ijms22168543 (Accessed: 19 July 2022).

Morris, G. M., Huey, R., Lindstrom, W., Sanner, M. F., Belew, R. K., Goodsell, D. S. and Olson, A. J. (2009) 'AutoDock4 and AutoDockTools4: Automated Docking with Selective Receptor Flexibility', Journal of Computational Chemistry, 30 (16), pp. 2785-2791. Wiley Online Library [Online]. DOI: https://doi.org/10.1002/jcc.21256 (Accessed: 15 November 2021).

Musuka, T. D., Wilton, S. B., Traboulsi, M., & Hill, M. D. (2015). Diagnosis and management of acute ischemic stroke: speed is critical. CMAJ : Canadian Medical Association journal = journal de l'Association medicale canadienne, 187(12), 887–893. [Online]. DOI: 10.1503/cmaj.140355 (Accessed: 19 July 2022).

Nakao, Y. and Fusetani, N. (2010) 'Marine Invertebrates: Sponges', Comprehensive Natural Products II, pp.327-362 [Online]. DOI: 10.1016/b978-008045382-8.00043-5 (Accessed: 1 August 2022).

Ördög, R. and Grolmusz, V. (2008) 'Evaluating Genetic Algorithms in Protein-Ligand Docking', In: Măndoiu I., Sunderraman R., Zelikovsky A. (eds) Bioinformatics Research and Applications, Lecture Notes in Computer Science, 4983. Springer Link [Online]. DOI: 10.1007/978-3-540-79450-9_37 (Accessed: 15 March 2022).

Orellana-Urzúa, S., Rojas, I., Líbano, L., and Rodrigo, R. (2020). Pathophysiology of Ischemic Stroke: Role of Oxidative Stress. Curr. Pharm. Des. 26, pp. 4246–4260 [Online]. DOI:10.2174/1381612826662007081339 12 (Accessed: 19 July 2022).

Patil, V., Balasubramanian, K. and Masand, N. (2019) Dengue Virus Polymerase, Viral Polymerases, pp. 387-428. [Online]. DOI:10.1016/b978-0-12-815422-9.00014-0. (Accessed: 19 July 2022).

Protein–Ligand Docking - Profacgen (2022), Profacgen.com. Available from: https://www.profacgen.com/protein-ligand-docking.htm (Accessed: 28 March 2022).

Sałaciak, K. and Pytka, K. (2022) 'Revisiting the sigma-1 receptor as a biological target to treat affective and cognitive disorders', Neuroscience & Biobehavioral Reviews, 132 pp.1114-1136 [Online]. DOI: 10.1016/j.neubiorev.2021.10.037 (Accessed: 19 July 2022).

Saliu, T., Umar, H., Ogunsile, O., Okpara, M., Yanaka, N. and Elekofehinti, O. (2021) 'Molecular docking and pharmacokinetic studies of phytocompounds from Nigerian Medicinal Plants as promising inhibitory agents against SARS-CoV-2 methyltransferase (nsp16)', Journal Of Genetic Engineering And Biotechnology, 19 (1). [Online]. DOI:10.1186/s43141-021-00273-5 (Accessed: 19 July 2022).

Schmidt, H., Zheng, S., Gurpinar, E., Koehl, A., Manglik, A. and Kruse, A. (2016) 'Human sigma-1 receptor bound to PD144418', [Online]. DOI: 10.2210/pdb5hk1/pdb (Accessed: 1 August 2022).

Trott, O. and Olson, A. J. (2009) 'AutoDock Vina: Improving the Speed and Accuracy of Docking with a New Scoring Function, Efficient Optimization, and Multithreading', Journal of Computational Chemistry, 31 (2), pp. 455-461. Wiley Online Library [Online]. DOI: https://doi.org/10.1002/jcc.21334 (Accessed: 15 November 2021).

Xing, C., Arai, K., Lo, E. and Hommel, M., 2012. 'Pathophysiologic Cascades in Ischemic Stroke', International Journal of Stroke, 7(5), pp.378-385. [Online]. (Accessed: 19 July 2022).

Xu, H., Wang, E., Chen, F., Xiao, J. and Wang, M., 2021. Neuroprotective Phytochemicals in Experimental Ischemic Stroke: Mechanisms and Potential Clinical Applications. Oxidative Medicine and Cellular Longevity, 2021, pp.1-45. [Online]. (Accessed: 19 July 2022).

Yang, Y., He, Y., Wei, X., Wan, H., Ding, Z., Yang, J. and Zhou, H. (2022) 'Network Pharmacology and Molecular Docking Based Mechanism Study to Reveal the Protective Effect of Salvianolic Acid C in a Rat Model of Ischemic Stroke'. Front. Pharmacol. 12, 799448. [Online]. DOI: 10.3389/fphar.2021.799448 (Accessed: 19 July 2022).